ELSEVIER

Contents lists available at ScienceDirect

Science of the Total Environment

journal homepage: www.elsevier.com/locate/scitotenv





Greenhouse gas production from an intermittently dosed cold-climate wastewater treatment wetland

S.H. Ayotte a,b,c, C.R. Allen b, A. Parker d, O.R. Stein b, E.G. Lauchnor b, E.G. Lauchnor b, C.R. Stein b, E.G. Lauchnor b, C.R. Stein b, E.G. Lauchnor b, C.R. Stein b, C.R. Stein b, E.G. Lauchnor b, C.R. Stein b, C.R. Stein

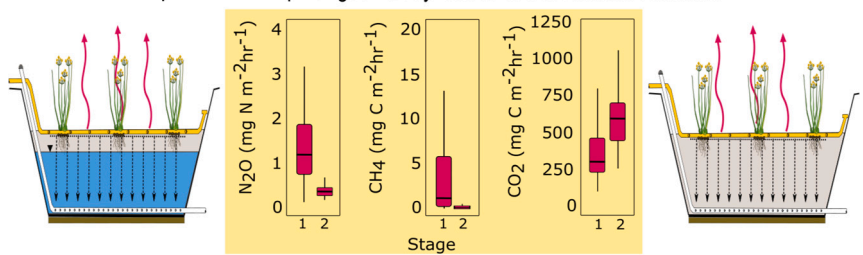
- ^a Center for Biofilm Engineering, Montana State University, Bozeman, MT 59717, USA
- ^b Department of Civil Engineering, Montana State University, Bozeman, MT 59717, USA
- ^c Thermal Biology Institute, Montana State University, Bozeman, MT 59717, USA
- ^d Department of Mathematical Sciences, Montana State University, Bozeman, MT 59717, USA

HIGHLIGHTS

- Emissions varied between the two stages with higher CH₄ and N₂O in the first stage.
- Fluxes of CH₄, N₂O and CO₂ significantly increased during wastewater doses
- Mass transfer effects may cause flux overestimates in intermittently dosed systems.
- High frequency of gas measurements is necessary to capture temporal variance.

G R A P H I C A L A B S T R A C T

Spatial and temporal gas flux dynamics of a Treatment Wetland?



Stage 1: Saturated, high organic carbon

Stage 2: Unsaturated, low organic carbon

ARTICLE INFO

Editor: Paola Verlicchi

Keywords: Nitrogen removal Constructed wetland GHG N₂O CH₄ CO₂

ABSTRACT

This study explores the greenhouse gas (GHG) fluxes of nitrous oxide (N2O), methane (CH4) and carbon dioxide (CO₂) from a two-stage, cold-climate vertical-flow treatment wetland (TW) treating ski area wastewater at 3 °C average water temperature. The system is designed like a modified Ludzack-Ettinger process with the first stage a partially saturated, denitrifying TW followed by an unsaturated nitrifying TW and recycle of nitrified effluent. An intermittent wastewater dosing scheme was established for both stages, with alternating carbon-rich wastewater and nitrate-rich recycle to the first stage. The system has demonstrated effective chemical oxygen demand (COD) and total inorganic nitrogen (TIN) removal in high-strength wastewater over seven years of winter operation. Following two closed-loop, intensive GHG winter sampling campaigns at the TW, the magnitude of N2O flux was 2.2 times higher for denitrification than nitrification. CH₄ and N₂O emissions were strongly correlated with hydraulic loading, whereas CO2 was correlated with surface temperature. GHG fluxes from each stage were related to both microbial activity and off-gassing of dissolved species during wastewater dosing, thus the time of sampling relative to dosing strongly influenced observed fluxes. These results suggest that estimates of GHG fluxes from TWs may be biased if mass transfer and mechanisms of wastewater application are not considered. Emission factors for N2O and CH4 were 0.27 % as kg-N2O-N/kg-TIN_{removed} and 0.04 % kg-CH4-C/kg-COD_{removed}. respectively. The system had observed seasonal emissions of 600.5 kg CO2 equivalent of GHGs estimated over 130-days of operation. These results indicate a need for wastewater treatment processes to mitigate GHGs.

^{*} Corresponding author at: Center for Biofilm Engineering, Montana State University, Bozeman, MT 59717, USA. *E-mail address:* ellen.lauchnor@montana.edu (E.G. Lauchnor).

1. Introduction

Treatment Wetlands (TWs), a type of constructed wetland, are an alternative to traditional mechanical wastewater treatment plants (WWTPs), combining mineral substrate, macrophytes, and microorganisms to improve water quality (Dotro et al., 2017). TWs rely on microbially mediated mechanisms similarly present in conventional WWTP for water quality improvements, and thus have the potential to emit greenhouse gases (GHGs) including nitrous oxide (N2O), methane (CH₄) and carbon dioxide (CO₂). Several recent studies have assessed microbially generated GHG emissions from WWTP with emissions ranging from less than one to over several hundred (mg m $^{-2}$ h $^{-1}$; Chen et al., 2020a; Fernández-Baca et al., 2018; Ma et al., 2011; Rodriguez-Caballero et al., 2015; Wang et al., 2019; Zhou et al., 2019). However, if TWs are to be considered a nature-based alternative to domestic wastewater treatment, GHG emissions from TWs must be compared to those from traditional and alternative nature-based treatment systems to assess their overall environmental impact.

Wastewater treatment in the United States (USA) is the second largest contributor of N_2O , accounting for 5.5 % of total USA N_2O emissions (EPA, 2022). The biotic and abiotic reactions that occur during the nitrification and denitrification processes are the primary mechanisms of N_2O production during wastewater treatment (Faulwetter et al., 2013, 2009). These processes have contributed to an increase in atmospheric N_2O concentration, from a stable 275 parts per billion (ppb) in the 18th century to 334 ppb by 2021, an 18 % increase (EPA, 2022; Nakazawa and Matsuno, 2020; Reay et al., 2012). Both conventional and nature-based wastewater systems can physically separate microbial processes with different oxidation-reduction requirements, such as nitrification and denitrification. This separation of processes allows for a more direct comparison of emissions, like N_2O , that can be generated by multiple distinct metabolic pathways.

Nitrification is a two-stage chemolithoautotrophic process mediated by two microbial symbionts that oxidize ammonia (NH₃) to nitrate (NO₃) via the intermediary nitrite (NO₂) (Shammas, 1986). N₂O production occurs during the first stage of this process when ammoniaoxidizing bacteria (AOB) oxidize NH3 to hydroxylamine (NH2OH). The intermediate oxidation of hydroxylamine by AOB forms the unstable intermediate nitroxyl (HNO) (Law et al., 2012) which can react with available NH2OH to form hyponitrous acid (H2N2O2). Hyponitrous acid then chemically decomposes to N2O (Chen et al., 2020a; Duan et al., 2018; Wunderlin et al., 2012; Zhu-Barker et al., 2015). N₂O production may increase exponentially with NH3 oxidation, as seen in a previous study (Law et al., 2012). One study reported that 86-96 % of the N2O produced during nitrification occurred during NH2OH oxidation (Tumendelger et al., 2019). Production of N2O by hydroxylamine oxidation is likely to occur under conditions of high NH₃ and low NO₃ which reflects influent domestic wastewater concentrations, indicating an opportunity for N2O efflux during nitrification.

Denitrification is a four-step dissimilatory reduction of nitrate (NO₃) to nitrogen gas (N2) by facultative anoxic heterotrophic bacteria. Different metabolic enzymes (nitrate reductase, nitrite reductase, nitric oxide reductase, and nitrous oxide reductase) catalyze each reduction step; N2O is produced from nitric oxide (NO) reduction and is an obligatory intermediate of denitrification (Chen et al., 2020a; Faulwetter et al., 2009; Wunderlin et al., 2012). Per Law et al. (2012), it was determined that the enzymatic reduction of N2O to N2 is almost four times faster than the rates of NO₃ or NO₂ reduction, suggesting that N₂O should not accumulate during heterotrophic denitrification. However, environmental factors and slower release of $\mathrm{N}_2\mathrm{O}$ reductase may result in transient accumulation of N2O (Law et al., 2012). Increased emissions of N2O in wastewater tend to result due to incomplete denitrification, which can be further exacerbated by high levels of NO₃, high temperatures, inadequate carbon to nitrogen (C:N) ratios, sudden changes in dissolved oxygen conditions and short retention times in the treatment process (Kaushal et al., 2014; Mander et al., 2011, 2021).

Methane produced during wastewater treatment accounts for 2.8 % of total US CH₄ emissions (EPA, 2022). In wastewater treatment, the production of CH₄ is linked to biogenic sources in treatment stages under highly reduced redox conditions and can account for an estimated 1 % of the influent COD load (Campos et al., 2016). CH₄ production likely occurs in TWs due to less stringent control of redox conditions in TW systems. Since CH₄ production prefers highly reduced conditions (-200 mV), anaerobic environments must be well established in TWs; intermittent loading and passive aeration may inhibit methanogenesis by increasing oxygenation of the system, resulting in CH4 oxidation (Dotro et al., 2017). During wastewater treatment, CO2 is the most emitted GHG (by volume) through heterotrophic respiration at both microbial and macrophyte levels (Oertel et al., 2016). However, equilibrium with the aqueous carbonate cycle may influence observed emissions and be attributed to the mineralization of organic carbon (Sharifian et al., 2021).

Many factors are correlated with TW GHG production, and findings are often contradictory. Temperature has been found to significantly impact N2O and CO2 emissions in constructed wetlands, with substrate and atmospheric temperatures positively correlated with emissions (Bahram et al., 2022; Jiang et al., 2020; Kaushal et al., 2014; Mander et al., 2021). However, the relationship between temperature and CH₄ flux is more complex. Only some of the studies conducted on TWs have found a positive correlation between wetland substrate temperatures and CH4 flux in wetlands treating domestic wastewater (Teiter and Mander, 2005). Several studies indicated that intermittent loading of TWs significantly increased N₂O (Hernandez and Mitsch, 2006, 2007) and CH4 flux relative to continuous loading but had limited to no effect on CO₂ emissions (Kaushal et al., 2014; Mander et al., 2011). Other studies suggest pulse loading decreased CH₄ flux (Altor and Mitsch, 2008). It is crucial to understand the impacts of environmental and operational factors on GHG emissions in TWs not only to compare to alternative systems, but also to both quantify GHG production and to discover potential operational controls that might minimize GHG emissions from TWs. Several previous studies have investigated GHG emissions from treatment wetlands, and to the best of our knowledge, no studies have considered the combined effects of pulse loading and low temperature operation on emissions (Kasak et al., 2022; Mander et al., 2008, 2011; Teiter and Mander, 2005). Additionally, no other studies have monitored GHGs from TWs with high frequency measurements capable of discerning temporal variation under rapidly changing environmental or operational factors.

This study investigates GHG emissions from an intermittently loaded two-stage vertical flow TW during winter when water temperature was approximately 3 °C. The system was designed for total nitrogen removal, with varying degrees of saturation to optimize for nitrification and denitrification processes. The primary objective of this research is to quantify low-temperature GHG production with a focus on N_2O emissions by nitrogen-removal processes associated with fixed biofilms in the TW. Our team predicts the production of GHGs follows patterns related to nutrient availability, controlled by intermittent wastewater application. For this study, two hypotheses are investigated: (1) Nitrifying bacteria produce similar N_2O emissions to denitrifying bacteria during low-temperature TW operation, and (2) the observed fluxes of N_2O , CH_4 , and CO_2 correlate with time of wastewater application.

2. Material and methods

2.1. Site description and system operation

Gas emissions and water quality analyses were performed at a pilot-scale TW operating in the winter season. The TW (Fig. 1) treats high-strength, domestic wastewater generated from toilets and kitchens at the Bridger Bowl Ski Area near Bozeman Montana USA (45°49'01.0" N $110^{\circ}54'21.8$ " W). Mean seasonal air temperature and annual snowfall at the studied TW were -4.7 °C and 6.2 m, respectively (Bridger Bowl Inc,

2023). The TW design is similar to a modified Ludzack-Ettinger process for advanced nitrogen removal (Metcalf, and Eddy, Inc. et al., 2014). It was designed as a two-stage, sub-surface vertical flow system where the first stage removes influent organic carbon (measured as chemical oxygen demand; COD) and denitrifies NO_3^- produced and recycled from the second stage. Each stage is comprised of two cells in parallel (area per cell, $A_C=23.8~\text{m}^2$; nominal depth, $d_o=0.9~\text{m}$). The first stage is saturated to a depth of 0.71 m which contains a treatment layer (nominal thickness =0.9~m) comprised of crushed gravel media ($d_{50}=5.3~\text{mm}$). The second stage is completely unsaturated containing a washed concrete-sand treatment layer (nominal thickness =0.9~m; $d_{50}=0.53~\text{mm}$). In both stages, the treatment layer sits over a 0.15 m drainage layer of coarser material and is covered with 0.1 m of crushed gravel media to provide insulation.

Influent wastewater first undergoes primary treatment in a series of sedimentation tanks. The primary treated influent is dosed to the first stage independently from doses of water recycled from the second stage. During the gas sampling campaign, the TW was treating 3.6 m³/d of influent and was operating at a 2:1 (recycle:influent) v:v ratio. The first stage received influent wastewater doses every 8 h, resulting in an areal dose depth of 2.5 cm (volume per dose, $V_{\text{dose}} = 1200$ L). The effluent of the second stage was recycled approximately every 90 min resulting in an areal dose depth of 0.8 cm ($V_{dose} = 400 \text{ L}$). The second stage received the mixed influent and recycled effluent from the first stage every 4 h, resulting in a 5.1 cm (V_{dose} = 2400 L) areal dose depth. Carex utriculata (sedge) and Scheneoplectus acutus (bulrush) were planted in 2013 and currently grow in the TW. Due to the lack of unplanted controls and the inability to install the gas sampling collars and caps over plants, offgassing from plants was not directly measured. Plants and their root exudates have been shown to alter subsurface microbial communities (Faulwetter et al., 2013), which may influence GHG production. The pore-space air in the non-saturated porous media was assumed to represent a bulk average of all processes occurring in the treatment media and provide representative flux measurements.

2.2. Gas flux measurements

Substrate gas fluxes were measured using the closed-loop dynamic chamber method with a Picarro G2508 (Picarro Inc., Santa Clara, CA, USA) gas analyzer. Eight locations in the TW (four each in the first and second stages; Fig. 1) were randomly selected to test spatial variability of gas fluxes from the stages assumed to perform predominantly denitrification (first stage) or nitrification (second stage), respectively. Any plant detritus was removed from the surface of the TW before inserting 20.3 cm diameter and 15.2 cm length polyvinyl-chloride (PVC) rings approximately 10 cm into the substrate a minimum of 24-h before sampling. The interior space of the ring was insulated with a 5 cm thick foam cap to maintain ground temperature and prevent snow accumulation on the exposed wetland substrate surface prior to sampling. Approximately 60 cm of snow was removed from the area surrounding the PVC collars prior to the start of each sampling campaign.

2.2.1. Manual sampling

In March 2022, gas efflux from the first (denitrification) and second (nitrification) stages in the system was monitored over three days by manually placing a chamber over the inserted rings (Fig. 1.). The chamber was made from a flat-bottomed polyvinyl chloride (PVC) endcap fitted with a rubber gasket along the bottom lip creating a tight seal with the ring (Fig. S1-S4). Two air-tight Swagelok® (Swagelok Co., Cleveland, OH, USA) sampling ports were located at the top of the chamber headspace and a pressure vent was located on the side of the chamber. Each chamber (volume of 0.0042 m³) covered a 0.032 m² substrate surface area. A closed loop was created by connecting the chamber to the Picarro G2508 gas analyzer with two 15 m lengths of 3.18 mm polyethylene-lined Bev A-line IV® Tubing (USP®, Lime, OH, USA) attached to the sampling ports. The Picarro G2508 gas analyzer, which uses cavity ring-down spectroscopy, monitored N2O, CH4, and CO2 gas concentrations at 1.17 Hz. Air in the chamber was circulated through the closed loop at a rate of 1.8 L min⁻¹ using a diaphragm pump

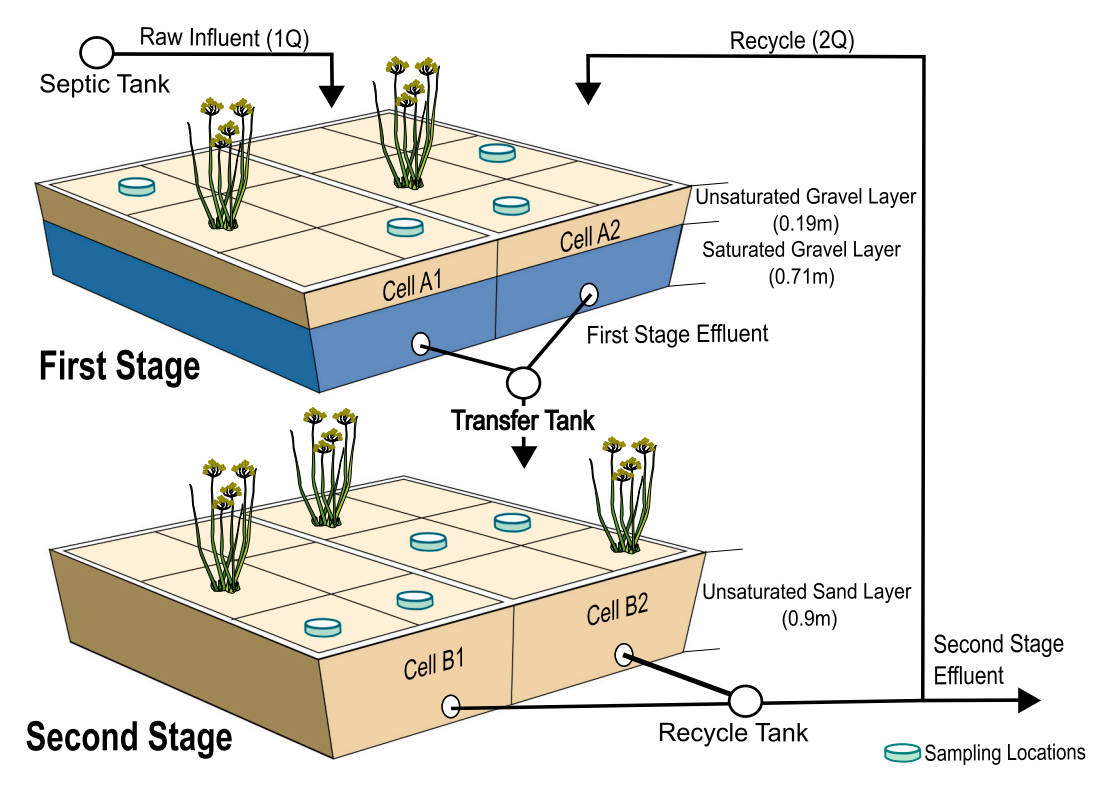


Fig. 1. Pilot TW System Schematic. Schematic of the TW system showing physical characteristics and randomly selected gas sampling locations. Cells in each stage are physically separated. Primary-clarified influent and recycle water are independently dosed onto the first stage at specified time intervals. For every volume of influent there were two volumes of recycled water over a 24 h period.

to prevent stratification and to establish continual mixing (Fig. S5).

Gas concentrations were measured by placing the chamber on a sample ring over an eight-minute sampling interval. The system was flushed with ambient air between each measurement. Sampling rotated between four locations in each stage (Fig. 1) in a recurrent pattern over a two-day (first stage) or one-day (second stage) period. A total of 40 sampling intervals (10 per location) in the first stage and 36 sampling intervals (9 per location) in the second stage were collected. The slopes of the gas concentrations over each eight-minute sampling interval were used to calculate fluxes as described in Section 2.4.

2.2.2. Automated sampling

In April 2022, a 48-h continuous monitoring at one location in the first (denitrification) stage assessed gas efflux patterns associated with intermittent dosing schedules. A Li-COR® 8100-103 Survey Chamber (volume of $0.0068\,\mathrm{m}^3$) replaced the manual chamber and was connected to the Picarro with two 30 m lengths of the Bev A-line IV tubing. The chamber closed automatically for a seven-minute read time. Flushing time with ambient air between measurements was 3 min, resulting in a frequency of six sampling intervals per hour. All other factors remained the same as described for manual sampling. The gas concentrations over time were collected to calculate gas flux, resulting in a total of 309 samples in April.

2.3. Ancillary measurements

Temperature measurements were collected via a thermistor located at the top of the LI-COR® survey chamber (8100-104 Thermistor, LI-COR®, Lincoln, NE, USA). Additional hourly temperature and pressure measurements were collected from the Bridger Base Area weather station (Bridger Bowl Inc., Bozeman, MT, USA). Water samples were collected from the influent, effluent of the first stage and final effluent from the system as either grab samples or as averaged composite samples over three-day periods. Continuous monitoring of the wetland water quality has occurred during the winter season for the past ten years (2013-present), and variability of nutrient parameters is consistently low once the system reaches a steady state (by January). COD was measured using HACH® digestion vials (HACH® Co., Loveland, CO, USA). A modified Berthelot reaction approach, as described by Rhine et al. (1998), was scaled to be performed in 96-well plates and used to determine ammonium (NH₄⁺-N₁ concentrations on a BioTek Synergy HTX Multimode Reader (Agilent Technologies, Inc., Santa Clara, CA, USA) at a wavelength of 660 nm. NO₃ and NO₂ were measured on a Metrohm Eco ion chromatograph with a Metrosep A Supp 5150/4.0 column, Metrohm Suppressor Module and 3.20/1.00 mM sodium bicarbonate/sodium carbonate eluent at 0.7 mL/min (Metrohm USA, Riverview, FL, USA). Total inorganic nitrogen (TIN) was defined as the summation of measured inorganic nitrogen species and was externally validated by MSU's Environmental Analytical Lab using a Shimadzu TOC-VSH (Shimadzu Scientific Instruments, Inc., Columbia, MD, USA).

2.4. Gas flux calculation and emission factor (EF)

Increases in gas concentration in the chamber headspace over each sampling interval were used to calculate gas fluxes by the linear approach described in Livingston et al. (2006). Quality control (QC) checks were completed on both the raw concentration data as well as the regressions of concentration over time. Raw data included 7- or 8-min sampling intervals. From these data, the initial 2 min were considered a stabilization period and removed from the determination of slope. Quality control checks were additionally performed on each of the 385 slopes calculated from the raw data. This QA/QC used the linear regression R^2 values for CO_2 measurements to assess goodness of fit. If the R^2 value for CO_2 was ≥ 0.9 , the slopes for all gases were accepted. Slopes for CO_2 with $R^2 < 0.9$ were removed from the dataset (Fig. S6). After quality control checks, a combined 368 slopes (95.56 %) were used

to calculate gas flux in March and April. The measured change of gas concentration versus time were combined with the measured chamber volume, ambient air pressure, chamber temperature and surface area to estimate the flux using Eq. (1).

$$J_c = \frac{V \bullet P_o}{R \bullet A \bullet (T + 273.15)} \bullet \frac{\partial C}{\partial t}$$
 (1)

where J_c is the gas efflux (mg m⁻² h⁻¹), V is the combined volume of the gas chamber and the tubing (m³), P_o is the ambient pressure (Pa), R is the gas rate constant (8.314 Pa m³ mol⁻¹ K⁻¹), A is the surface area of the chamber (m²), T is the initial chamber air temperature (°C), and $\frac{\partial C}{\partial t}$ is the rate of gas accumulation over time, expressed as a gas mole fraction (µmol mol⁻¹ s⁻¹).

The emission factor (EF) is a measure of the ratio of GHG produced relative to the daily mass of nitrogen or carbon removed (kg $\rm N_2O\text{-}N/kg$ $\rm TIN_{removed}$; kg CH₄-C/kg COD_{removed}) and is reported as a percentage or fraction (IPCC, 2019). The IPCC (2019) has not officially specified whether the total load or mass removal should be used to determine the EF. For this paper, the treated or removed mass of carbon or nitrogen was used to determine the EF. The EFs were calculated for CH₄ and N₂O using the Tier I approach by IPCC (2019) as shown in Eqs. (2) and (3) and compared various wastewater treatment facilities and constructed wetlands.

$$EF = \frac{(J_{N_2O-N} \bullet A)}{(TIN_{in} - TIN_{eff})}$$
 (2)

$$EF = \frac{(J_{CH_4-C} \bullet A)}{(COD_{in} - COD_{eff})}$$
(3)

where EF is emission factor of the gas of interest expressed as a mass ratio (kg / kg removed), $J_{\rm N2O-N}$ is the N_2O gas flux from system (kg $N_2O-N\,m^{-2}\,day^{-1})$, $J_{\rm CH4-C}$ is the CH4 gas flux from system (kg C m $^{-2}\,day^{-1})$, A is the total surface area of the TW system (47.6 m² per stage), TIN_{in} is the influent daily mass flux of total inorganic nitrogen through the system (kg day $^{-1}$), TIN_{eff} is the effluent daily mass flux of total inorganic nitrogen (kg day $^{-1}$), COD_{in} is the influent daily mass flux of COD (kg day $^{-1}$), and COD_{eff} is the effluent daily mass flux of COD (kg day $^{-1}$). Daily mass flux of TIN and COD were calculated as the product of aqueous concentrations (mg L^{-1}) and the system's daily volumetric flow rate (m³ day $^{-1}$) after unit conversions.

The EF was not determined for CO_2 due to the IPCC (2019) guidance that determined organic carbon found in domestic wastewater to be from modern organic matter found in human excrement and is thus considered to be predominantly biogenic. Consequently, since this carbon is not related to the transfer of ancient carbon stores from the lithosphere to the atmosphere, reporting CO_2 emission factors from domestic wastewater is currently excluded from GHG inventories (IPCC, 2019). Additionally, no supplemental carbon was added to the system and this study considered only the measured direct emissions from the TW surface, excluding any potential non-biogenic sources that would be used to calculate a CO_2 EF according to current reporting standards (IPCC, 2019).

The CO_2 -equivalent (CO_{2eq}) was determined using each GHG's global warming potential (GWP). A 100-year GWP of 27 and 273 were used for CH₄ and N₂O, respectively (IPCC, 2021). Eq. (4) shows how the CO_{2eq} was determined:

$$CO_{2_{eq}} = J_c \bullet \frac{MW}{AW} \bullet GWP \tag{4}$$

where CO_{2eq} is the carbon dioxide equivalent (mg $CO_2e\ m^{-2}\ h^{-1}$), MW is the molecular weight of the compound of interest (CH₄, N₂O or CO₂; mg/mmol), AW is the atomic weight of the element of interest (C or N; mg/mmol), and GWP is the 100-year global warming potential of CH₄ or N₂O (mg CO_2 /mg GHG).

2.5. Data analysis

R version 4.2.1 (R Core Team, 2022) was used to analyze and visualize all data. Analysis of covariance (ANCOVA) investigated spatial influences on gas flux, such as system stage, and sample location. Interactions between time*stage and time*location were assessed in separate ANCOVA models to account for temporal effects.

Generalized Additive Models (GAM) were used to model temporal trends associated with intermittent dosing schedules. GAM uses smoothers to uncover nonlinear relationships with covariates (Hastie and Tibshirani, 1986) and was essential for determining patterns within our dataset. The package "mgcv" (Wood, 2017, 2011) was used to fit GAMs with tensor product interactions and P-splines, as proposed by Eilers and Marx (1996). The restricted maximum likelihood (REML) approach was used to provide unbiased estimates by accounting for loss in degrees of freedom from estimating fixed effects (Harville, 2023). A flux was calculated by Eq. (1) every 10 min after each wastewater dose (primary-clarified influent or recycled effluent). Measurements were grouped into eight-hour blocks determined by the occurrence of an influent dose. GAMs were fit to N2O, CO2 and CH4 fluxes with smoothers for absolute time, time after the influent dose and time after the recycle dose. N₂O and CO₂ models additionally included chamber temperature; however, chamber temperature did not strongly influence CH₄ flux (p > 0.05) and was not included in that model. Imputation was used to assure time points at 10-min intervals which allowed an auto-regression and moving average (ARMA) time series model to be fit. Gas flux was logtransformed for all analyses to meet Gaussian and constant variance assumptions. All model assumptions were met and validated using diagnostic plots of residuals, including Autocorrelation Function and Partial Autocorrelated Function plots to assess ARMA model fit. For each GAM-ARMA fit, the Benjamini-Hochberg method was applied to maintain a family-wise false discovery rate of 5 % ($\alpha = 0.05$).

3. Results

During March and April of the 2021–22 operational season, the TW removed COD, TIN and NH $_3$ from the influent wastewater, with results averaged from 20 samples provided in Table 1. Influent concentrations of COD (808 mg L $^{-1}$) and TIN (161 mg L $^{-1}$) were higher than typical domestic wastewater due to the lack of laundry and shower facilities at the resort. The system removed an average of 96.6 % influent COD. The TW removed nearly 3/4 of the total inorganic nitrogen (NH $_4^+$ -N, NO $_3^-$ -N, and NO $_2^-$ -N), removing 74.3 %. Ammonium levels in the second-stage effluent were consistently below the detection limit of <0.1 mg L $^{-1}$ NH $_4^+$ -N, resulting in >98 % removal of NH $_4^+$ -N. The first stage also exhibited an average of 73.7 % NO $_3^-$ -N and 24.6 % NH $_4^+$ -N removal. Nitrate was added to the first (denitrification) stage via recycle from the second (nitrification) stage effluent at twice the influent flow rate, resulting in an average of 26 mg L $^-$ 1 NO $_3^-$ -N applied to the first stage at a one-part influent to two-part recycle ratio.

3.1. First stage vs. second stage gas flux – March sample campaign

The median GHG fluxes (Table 1) from the first stage were 0.66 mg N_2 O-N m⁻² h⁻¹, 0.85 mg CH₄-C m⁻² h⁻¹, and 221 mg CO₂-C m⁻² h⁻¹. Median second stage emissions were 0.34 mg N_2O-N m⁻² h⁻¹, 0.2 mg CH₄-C m⁻² h⁻¹, and 606 mg CO₂-C m⁻² h⁻¹. Fig. 2 illustrates the variability of N2O, CH4, and CO2 gaseous efflux at each sampling location in March 2022. The ranges of fluxes in March were 0.025-4.66 mg N₂O-N $m^{-2} h^{-1}$, 0.029–28.07 mg CH₄-C $m^{-2} h^{-1}$, and 81.10–1062.49 mg CO₂-C m⁻² h⁻¹. Since samples were collected over the course of several days, a two-way ANCOVA with a time dependent interaction was used to model the data. Sample locations within each stage had no statistically significant difference in emissions ($p \ge 0.16$). Although there was not a significant difference, the proximity of a sample location to a dosing orifice may explain increased variability of emissions at that location. Emissions of N2O, CH4 and CO2 were found to be different between stages ($p \le 0.05$). The first stage of the system, where denitrification and potentially methanogenesis occur, produced greater emissions of the more potent greenhouse gases, N2O and CH4 (Fig. 2). Conversely, the second stage, designed primarily for nitrification, emitted more CO₂, despite lower influent COD levels. The median N2O and CH4 flux were respectively 2.2 times and 4.8 times greater in the anoxic first stage than the aerobic second stage, while CO2 efflux was 2.46 times greater in the second stage. Higher emissions in the first stage were generally observed immediately after active dosing, suggesting that the temporal variability in gas fluxes was related to the time of the sampling interval relative to the dosing schedule. Other studies have noted high variability of gas emissions in intermittently dosed wetlands (Ji et al., 2021; Mander et al., 2014, 2011), but have not considered instantaneous shifts in emissions relative to dosing.

3.2. Temporal fluctuations with hydraulic loading - April sample campaign

To further understand temporal dependence, a 48-h continuous monitoring of one location in the denitrifying stage was conducted in the first week of April 2022. Frequent flux measurements at a single location and over a longer duration provided more clarity to observe trends. For reference, the first stage received primary-treated influent doses every 8-h, with recycle doses loaded six-times over each 8-h cycle, resulting in a periodic introduction of organic carbon 3-times per day and NO_3^- 18-times per day. The second stage received NH_4^+ rich doses every 4-h (6 times per day). Emissions from the second stage in March indicated no statistically significant differences ($p \geq 0.06$) with time; therefore, temporal trends of emissions were considered only in the first stage.

The calculated gas flux and temperature exhibited trends with high variability over the 48-h period at one location in the first stage (Fig. 3). Temperature in the air and the chamber varied over the sampling period from a low of $-9\,^{\circ}\mathrm{C}$ to a high of 13 $^{\circ}\mathrm{C}$. As expected, large peaks of $N_2\mathrm{O}$ and CH_4 flux corresponded to influent doses, other peaks in $N_2\mathrm{O}$ and CO_2 generally aligned with the smaller recycle doses. Gas fluxes during the April sampling campaign ranged from 0.067 to 6.03 mg $N_2\mathrm{O-N}$ m $^{-2}$ h $^{-1}$, 0.065–61.71 mg CH_4 -C m $^{-2}$ h $^{-1}$, and 27.38–927.27 mg CO_2 -C m $^{-2}$

Table 1
Mean pollutant concentrations (w/ standard deviation) in the influent and effluent of the system stages and median flux (w/ 95 % confidence intervals) for March–April 2022.

	Stage	COD	NH ₄ -N	NO ₃ -N	TIN	CO ₂ flux	CH ₄ flux	N ₂ O flux	
		(mg L^{-1})	(mg L^{-1})	(mg L^{-1})	(mg L ⁻¹)	$(mg C m^{-2} h^{-1})$	$(mg C m^{-2} h^{-1})$	(mg N m ⁻² h ⁻¹)	
Influent		808 (59.3)	161 (26.6)	0.4 (0.3)	161 (26.9)				
Effluent	First	52 (10.8)	45 (11.3)	5.0 (4.0)	45 (11.3)	221 (211-230)	0.85 (0.77-0.93)	0.66 (0.63-0.69)	
Effluent	Second	28 (3.8)	$0.707^{\rm b}$	39.0 (4.0)	39 (4.0)	606 (359–853)	0.2 (0.02-0.39)	0.34 (0.17-0.51)	
Total Removal (%) ^a		97 %			74 %				

^a Calculated based on daily mass loading.

^b Measured values below detection limit, estimated using [MDL/ ($\sqrt{2}$)] (Croghan and Egeghy, 2003).

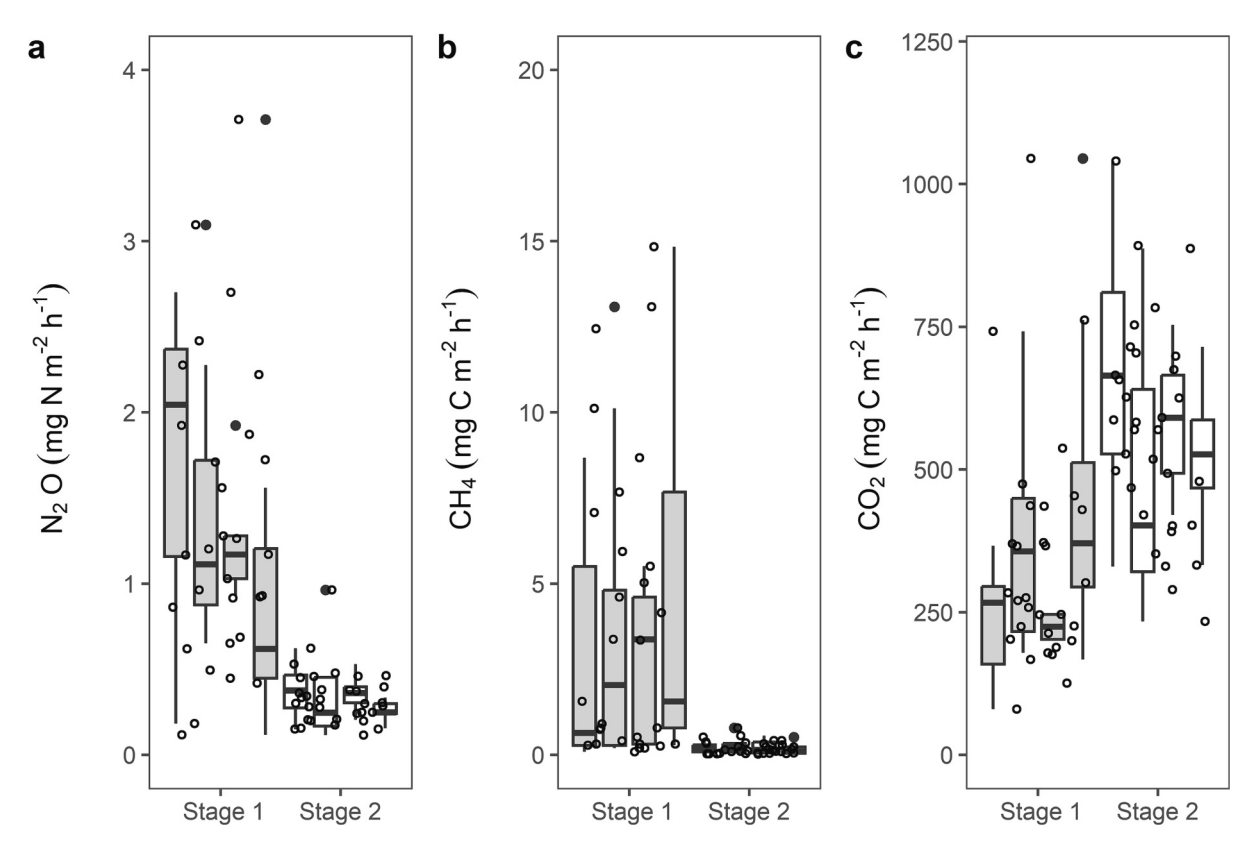


Fig. 2. Flux distributions for N_2O , CH_4 and CO_2 by stage and sample location. The bar in the center indicates the median flux. The upper and lower reaches of the boxes indicate the upper (75th) and lower (25th) quartiles of the fluxes (interquartile range – IQR), and the whiskers represent the minimum and maximum up to $\pm 1.5^*$ IQR. Dots indicate calculated flux values, and points that extend beyond the whiskers are potential outliers. There was no statistically significant difference in median emissions between locations within a stage ($p \ge 0.05$).

 $h^{-1}.$ The median values were 0.66 mg $N_2 O\text{-N}$ m $^{-2}$ $h^{-1},\,0.85$ mg CH₄-C m $^{-2}$ $h^{-1},\,$ and 221 mg CO₂-C m $^{-2}$ $h^{-1}.$ The median and variance of $N_2 O$ and CH₄ emissions were higher than observed from the first stage in March, perhaps due to the tighter sampling frequency picking up higher emissions around the timing of a dose.

The calculated fluxes were modeled by a GAM-ARMA that shows the overall smoothed trends over the dose cycles and corresponds to the intermittent loading of wastewater (Fig. 4). The GAM highlights the temporal variability due to the dose schedule.

3.2.1. Nitrous oxide emissions

 N_2O exhibited strong trends with dosing schedules (Fig. 4a). The median N_2O flux across all cycles for the first hour after an influent dose high in COD was 0.78 mg $N_2O\text{-N}$ m $^{-2}$ h $^{-1}$ (95 % CI: 0.66–0.92). The flux then decreased by 76 % (p < 0.001) during hour two across all cycles to a minimum value of 0.19 mg $N_2O\text{-N}$ m $^{-2}$ h $^{-1}$ (95 % CI: 0.16–0.22). A steady linear increase was observed from hours two to five (p < 0.05), followed by a stable period of flux (p > 0.05) from hours five to eight with a median flux of 0.99 mg $N_2O\text{-N}$ m $^{-2}$ h $^{-1}$ (95 % CI: 0.94–1.03). Secondary peaks were noted throughout the 8 h and corresponded to the onset of each recycle dose, which contained high concentrations of NO_3^- (dose intervals not shown). The differences in median N_2O flux between cycles were strongly correlated to temperature effects (Fig. 3). Cycles with similar average temperatures resulted in N_2O fluxes that were not greatly different (p > 0.05).

3.2.2. Methane emissions

The gas efflux of CH₄ was at a maximum at the start of each influent dose cycle and displayed a general exponential decrease thereafter (Fig. 4b). In the first hour of each cycle, the median flux was 9.24 mg CH₄-C m $^{-2}$ h $^{-1}$ (95 % CI: 7.5–11.3) which rapidly decreased to 5.4 mg

CH₄-C m⁻² h⁻¹ (95 % CI: 4.4–6.5) by the second hour, a decline of 41.5 % (p < 0.001). By hour seven, the flux reached a steady state of 0.18 mg CH₄-C m⁻² h⁻¹ (95 % CI: 0.15–0.21), which was 2 % of the initial flux. A comparison of the median flux between each hour within a cycle showed that all hours were significantly different (p < 0.001), except for hours seven and eight, which corresponded to the steady state flux at the end of the cycle. The high initial rates of CH₄ emissions were linked to the large influent wastewater doses. Median fluxes over entire dose cycles ranged from 0.70 to 1.12 mg CH₄-C m⁻² h⁻¹.

3.2.3. Carbon dioxide emissions

Spikes in CO₂ emissions corresponding to both the three influent doses and the eighteen recycle doses per day are apparent, but repeating patterns of CO₂ emissions within the 8-h influent dose cycle were not as obvious as those observed for N₂O and CH₄ (Fig. 4c). The six eight-hour cycles were compared using a paired-mean comparison approach and data were grouped into cycles numbered chronologically one to six (Fig. 4c). A moderate decrease with time within the cycle was observed across all cycles except cycle three, the only cycle in which the surface temperature steadily increased throughout the 8-h period (Fig. 3). Median CO_2 fluxes for cycles one, three, five, and six were not different (p >0.05), however, the median values for cycles two and four were significantly different from the other four (p < 0.05), in a pattern similar to the findings for N2O. Cycle 2 had both the lowest emissions and lowest average temperature, cycle 4 had the highest emissions and highest temperature and median values over a cycle strongly correlated to surface temperature (p < 0.001). The initial median CO_2 flux at the start of a cycle was calculated to be 275.1 mg CO₂-C m⁻² h⁻¹ (95 % CI: 246.7–306.7), which then decreased by 35.1 % (p < 0.001) to a median of 178.5 mg CO_2 -C m⁻² h⁻¹ (95 % CI: 161.8–197.0) by the eighth hour.

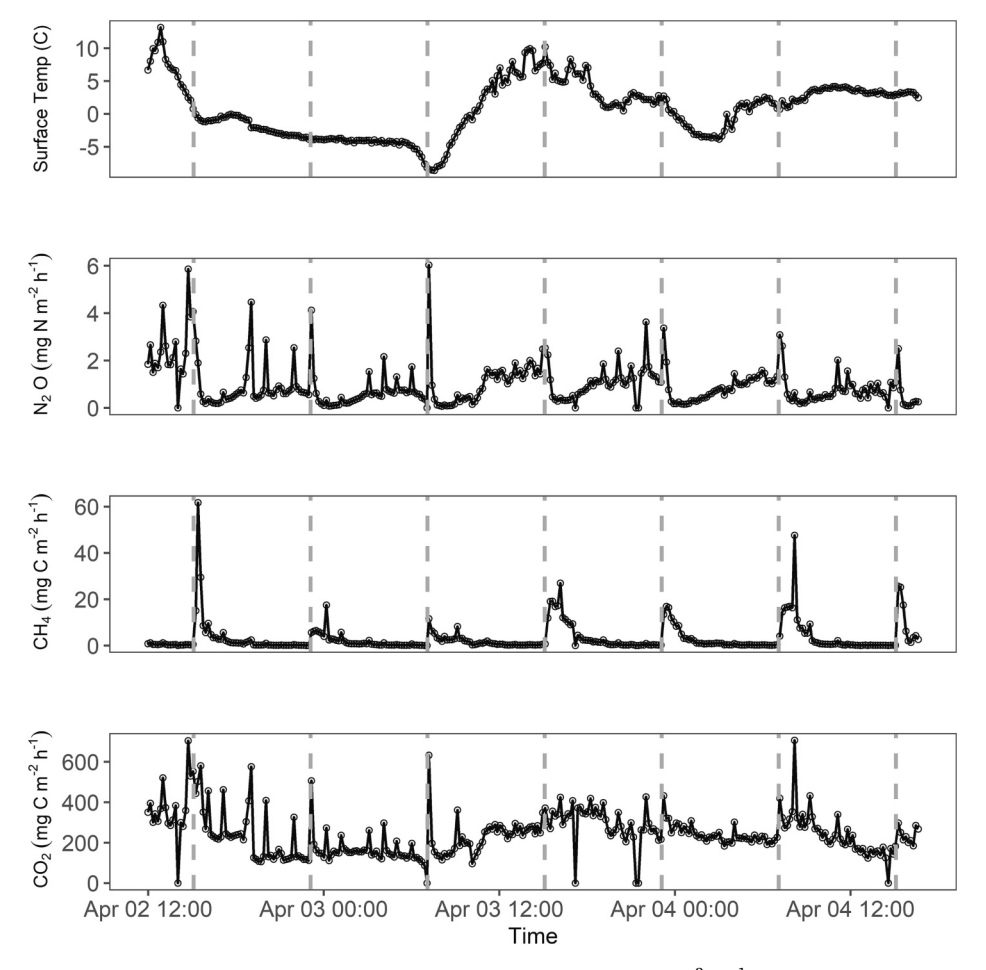


Fig. 3. Flux and Temperature data in the system's first stage. N_2O , CO_2 and CH_4 gas flux (mg-N or C m⁻²·hr⁻¹) in the denitrification stage of the pilot TW plotted with surface temperature. Measurements were recorded over a 48-h period, at a frequency of 6 measurements per hour. Dashed vertical lines indicate the occurrence of a primary-clarified influent wastewater dose onto the wetland (~750 mg L⁻¹ COD). Lines connecting points represent piecewise linear trends visualized using the R ggplot() function.

3.3. Global warming potential and emission factors

For estimates of seasonal emissions, the Global Warming Potentials (GWP) as CO_2 equivalents (IPCC, 2021) were determined for the GHGs across the entire TW system using Eq. (4). Daily, the TW system contributed 1.0 kg of CO_{2eq} of $\mathrm{N}_2\mathrm{O}$ and a combined CH_4 and CO_2 of 3.5 kg CO_{2eq} . Over the 2021–2022 ski season, the total estimated GWP of the TW was 600.4 kg of CO_{2eq} assuming 130-days of operation, of which CH_4 and $\mathrm{N}_2\mathrm{O}$ emissions accounted for 0.9 % and 24.2 %, respectively.

Emission factors of GHG are typically determined by the ratio of mass emitted per mass removed as nitrogen or carbon (for example: kg $N_2O-N/\ kg$ TIN-N removed) (Foley et al., 2010). However, EF is not a standardized metric and is often provided in terms of influent daily mass, which can influence the EF value (Tumendelger et al., 2019). Emission factors used in this study were standardized to carbon and nitrogen daily mass removal. The studied TW had a system EF of 0.04 % and 0.27 % for CH₄ and N_2O_1 , respectively.

4. Discussion

4.1. Water quality

The TW effectively removed influent nitrogen and COD to similar or better levels than more energy- and labor-intensive mechanical systems. Pollutant removal efficiencies in the studied system met or exceeded discharge requirements set by the Montana Department of Environmental Quality for Level II treatment systems, which require oxidation of NH $_4^+$ and 60 % total nitrogen (TN) removal. Removal of NH $_4^+$ in the pilot system corresponded to treatment efficiencies observed in full-scale mechanical wastewater treatment facilities, such as a conventional activated sludge (CAS) system and a modified Ludzack-Ettinger (MLE) system (Table 2) which removed 98.2% and 91.6 % of NH $_3$ (Tumendelger et al., 2019). The mean removal efficiencies of COD and TIN in the studied TW (Table 1) were similar to a hybrid-constructed wetland treating anaerobic digestate, which removed 72.5 % and 94.6 % of COD and TN, respectively (Zhou et al., 2020). Both TW systems treated concentrated influent, with NH $_4^+$ levels of the studied TW between two and eight times higher than typical domestic wastewater (Henze, 2008).

4.2. Emission factors

The emission factor for N_2O , which was 0.27 % (Table 2), was only minimally lower than emissions from a similarly designed hybrid TW treating anaerobic digestate, with an EF_{N2O-N} of 0.34 % (Zhou et al., 2020). If only TIN loading was accounted for, the EF_{N2O-N} of the TW was 0.21 %, which is only slightly lower than the EF value determined based on removal. The EF_{N2O-N} for the studied TW fell within the reported range of various TWs; however, traditional full scale WWTPs emitted two to twelve times more N_2O than the studied system. EF_{N2O-N} values calculated in terms of influent TN are indicated with the letter 'C' in Table 2. Only a few studies reported the EF for CH₄ (Table 2); however,

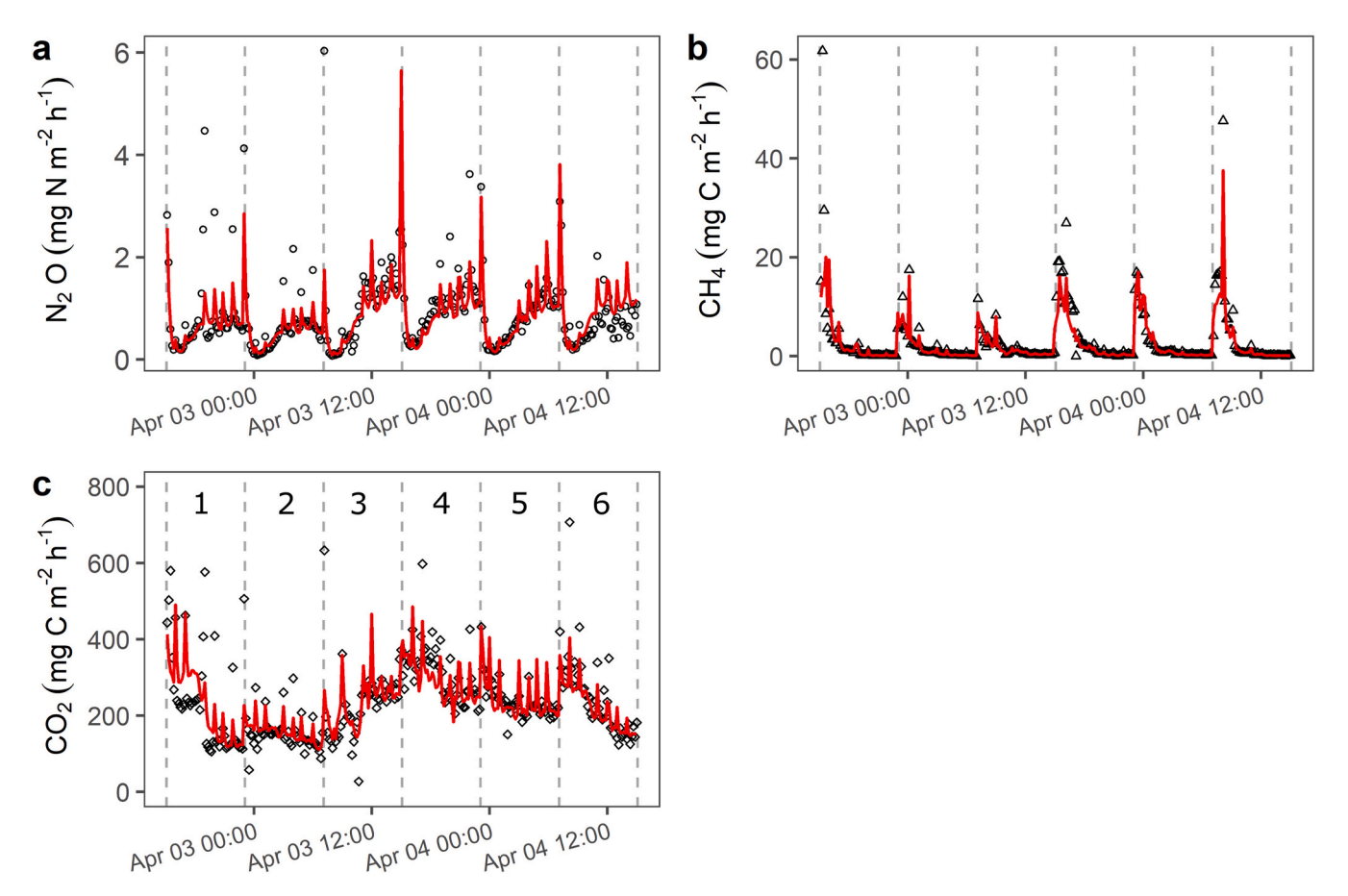


Fig. 4. GAM fit of gas fluxes. GAM fit of N_2O (a), CH_4 (b), and CO_2 (c) soil efflux over six continuous 8-h cycles defined by an influent dose. Numbers 1–6 for CO_2 indicate cycle number. Dashed vertical lines indicate occurrence of an influent wastewater dose. Six recycle doses (not plotted) generally correspond with smaller intermediate peaks.

the range of CH₄ emissions was heavily skewed by whether EF was calculated based on influent carbon or overall removal. Based on these results, the studied TW appears to generate less N2O and CH4 than most mechanical treatment plants. Additionally, some studies have reported that macrophytes in wetlands can affect GHGs depending on plant species (Chen et al., 2020b; Faulwetter et al., 2009; Hernández et al., 2018; Jiang et al., 2020; Mander et al., 2014, 2021; Maucieri et al., 2019). One study estimated that in optimal conditions, anywhere from 1.56×10^{-2} to 2.08×10^{-2} kg CO₂-C m⁻² day⁻¹ may be assimilated by plants (Mander et al., 2008). In Montana, the typical growing season is 135 days or less (Western Agricultural Research Center, 2019), resulting in the potential sequestration of 181.8 to 243.4 kg CO₂ per 135-days or 30-40 % of the generated CO_{2eq} during our winter operation (~91 % plant coverage from a 2022 survey of the pilot TW). However, assimilation is typically unstable and may be easily mineralized when the water table is lowered (Mander et al., 2014). Research of TW mesocosms indicated that plants universally increased CO2 emissions, regardless of season (Allen, 2016). As a result, the studied TW is more likely a net emitter of CO₂ than a sink. Since this study was performed during plant senescence, uptake and active transport of gas by plants was assumed to be negligible. The effect of plants on passive movement of gases in TWs due to open stomates and broken stems has been hypothesized (Armstrong, 2000; Verboven et al., 2014), but was beyond the scope of this investigation. Future studies on systems operating over an annual plant growth cycle and with unplanted controls would be necessary to accurately evaluate plant impact on the release of the GHGs studied here.

4.3. Production vs emissions

Often GHG emissions are assumed to be produced at the location of measurements (Mander et al., 2014). However, in TWs and wastewater treatment systems, convective transport and aqueous water chemistry may play a bigger role than often considered. As shown in Fig. 5, the hydraulic design of TWs may result in physical mechanisms that increase emissions via mass transfer, including 1) the volatilization of dissolved gases at the dosing orifices, 2) the displacement of gas in the unsaturated porous media by large volume doses, and 3) the release of large concentrations of dissolved gases when the gas-liquid surface area increases in unsaturated or aerated systems (Bruun et al., 2017; Doran, 1995; Foley et al., 2010; Law et al., 2012; Sharifian et al., 2021; Tumendelger et al., 2019). Mass transfer effects may cause incorrect assumptions of where the GHG is generated across wastewater systems, leading to over or underestimations of production by different microbial processes. Interestingly, most studies link the increased emissions from intermittent dosing to biological factors such as nitrification and denitrification. However, physical processes associated with mass transfer, displacement, and off-gassing likely confound changes in emissions. The effect of mass transfer on GHGs is discussed in Sections 4.3.1-4.3.3.

4.3.1. Nitrous oxide

The mostly anoxic first stage of the wetland effectively contributed 68.8~% of the total N_2O emissions from the system corresponding to the common paradigm that N_2O is predominantly generated by anoxic denitrification (Meyer et al., 2005; Velthuis and Veraart, 2022; Vilain et al., 2014). While emissions in the second stage were likely due only to nitrification, NH_3 removal in the first stage indicated that while

Table 2
Mean influent water quality (sd) and greenhouse gas emission factors from systems treating domestic wastewater.

System type	Location	Wastewater	$\frac{Q}{(m^3 d^{-1})}$	COD	TOC	(g-N m ⁻³)	EF _{CH4-C} (%)	(%)	Reference
		description		(g m ⁻³)	(g m ⁻³)				
Constructed wetlands									
Two stage VSSF	Montana, US	Pre-settled municipal	3.6	808.3 (59.3)	268 (17.4)	161 (26.9)	0.04 %	0.27 %	This Study ^a ,
Hybrid VSSF/HSSF	China	Swine anaerobic digestate	3.6	2725 (1264)	909 (420.3)	379 (58)	n.a	0.34 %	[1] ^{b,c}
Hybrid VSSF, HSSF and two FWS	Estonia	Raw municipal	11.3	n.a.	16.1	50.9	0.88 %	0.021 %	[2] ^d
HSSF, planted sand filter	Estonia	Hospital	n.a.	n.a.	69.0	109.0	9.9 %	0.45 %	[2] ^d
FWS	Sweden	Secondary municipal	264	n.a.	n.a.	237.0	0.25 %	n.a.	[3]
Mechanical wastewater tre	eatment								
CAS	Germany	Municipal	5000	746.6	n.a.	52.8	0.01 %	0.001 %	[4] ^c
MLE	Germany	Municipal	14,600	202.2	n.a.	83.0	0.004 %	0.008 %	[4] ^c
MBR	Washington, US	Municipal	62,000	283 (40)	n.a.	52 (7.9)	n.a.	0.60 %	[5]
CAS	QLD, Australia	Municipal	5000	499 (104)	n.a.	64.0 (6.5)	n.a.	1.90 %	[6] ^c
MLE	Western Australia	Municipal	63,000	730	n.a.	50	n.a.	2.70 %	[7]
SBR	Western Australia	Municipal	137,000	550	n.a.	47-58	n.a.	3.27 %	[7]
"A ² /O"	New South Wales (Cavanaugh, 2021)	Municipal	25,000	850	n.a.	55–85	n.a.	1.40 %	[7]
MLE	South Australia	Municipal	49,000	700	n.a.	69-103	n.a.	3.57 %	[7]

- 1 (Zhou et al., 2020).
- 2 (Teiter and Mander, 2005).
- 3 (Johansson et al., 2004).
- 4 (Tumendelger et al., 2019).
- 5 (Cavanaugh, 2021).
- 6 (Pan et al., 2016).
- 7 (Foley et al., 2010).
 - ^a Total inorganic N.
- ^b TOC estimated from COD.
- ^c EF reported per kilogram of influent N and C.
- ^d EF reported per kilogram of TOC removed.

denitrification dominated, NH_3 removal also contributed to TIN removal and likely N_2O emissions. Traditional mechanical wastewater treatment plants comparatively observe the opposite trend, where substantially higher emissions of N_2O are measured in aerated nitrification reactors. For example, one MLE in Ruelzhiem, Germany, found that 21.1 % of emissions were associated with nitrification, whereas only 7 % were associated with denitrification (Tumendelger et al., 2019). Additional studies have found that N_2O emissions were approximately 2–3 times greater in reactors undergoing active aeration (Law et al., 2012). Active aeration, paired with the high mass transfer coefficient of N_2O , may quickly strip any generated N_2O to the atmosphere resulting in greater observed emissions (Foley et al., 2010).

The temporal trends associated with N2O in the first stage may be linked to mass transfer rather than changes in the biological production of the gas. During dosing of influent wastewater, in which dissolved N2O gas is likely minimal, we noted relatively large peaks in the N2O flux. During these instances, it is hypothesized that N₂O accumulated in the unsaturated porous volume of the gravel media (top 0.19 cm of first stage) and was displaced by the doses, as described in mechanism 2 (Fig. 5). Influent doses (2.5 cm dose depth) displace approximately 30 % of the unsaturated gravel pore space, assuming a conservative 40 % porosity, potentially resulting in a large flushing of N₂O gas to the atmosphere. The same mechanism could also explain the smaller peaks in flux associated with the smaller (0.8 cm) recycle doses which displace approximately 10 % of the pore volume. Other studies of wetlands have noted significant increases in N2O emissions due to pulse loading hydrology (Mander et al., 2011); while another study reported seeing no impact on the total net export of N2O (Bruun et al., 2017). Mander et al. (2011) suggested that the length and frequency of individual doses may

be the reason for contradictory findings.

4.3.2. Methane

The average CH₄ flux from the first stage was 4.9 times greater than that observed from the second stage, which may be attributed to differences in organic carbon loading, degree of saturation in the first stage that favors anaerobic processes such as methanogenesis or volatilization of dissolved gases at the dosing orifices. The rapid increase and subsequent decrease of CH₄ emissions from the first stage (Fig. 4b) suggests that dissolved CH₄, likely produced in the septic tank, was off-gassed during doses as described in mechanism 1 (Fig. 5). One study reported approximately 1 % of influent COD may be converted to CH4 in the anaerobic sewer distribution system (Campos et al., 2016), and others have reported high dissolved CH₄ concentrations in influent wastewater suggesting that CH₄ may be transported and off-gassed from preceding stages (Tumendelger et al., 2019). Mander et al. (2011) observed 7-12 times higher CH₄ emissions from TWs that were intermittently loaded or had fluctuating water tables compared to systems with constant water tables. In all these studies, large increases in CH₄ emissions appear to be attributable to mass transport and ebullition. The low observed CH₄ fluxes by hour two of each cycle in the present study are likely more indicative of the inherent methanogenic capacity of the first stage, but measurement of dissolved gases in future investigations will be needed to confirm this hypothesis. Ultimately, release of CH₄ from the influent water may overestimate emissions actively produced in the wetland but are representative of the CH₄ generation across the entire wastewater treatment system.

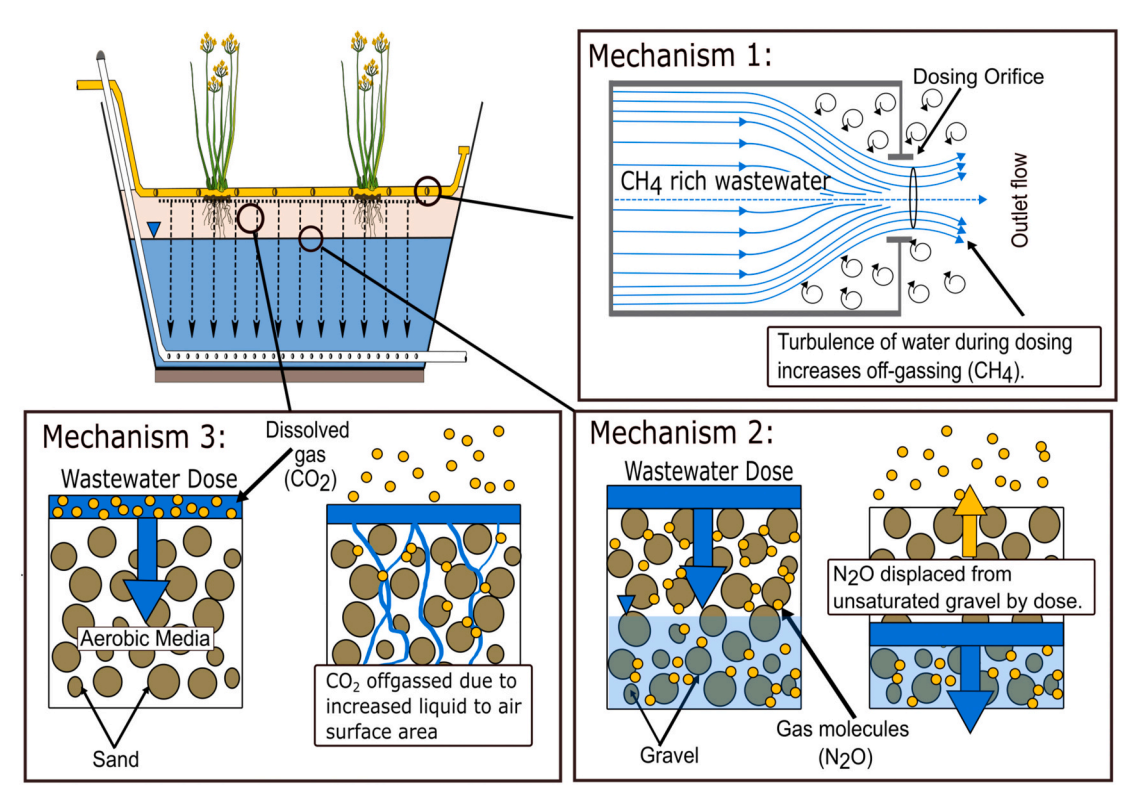


Fig. 5. Emissions due to physical mechanisms. Physical mechanisms that increase emissions via mass transfer, including 1) the volatilization of dissolved gases at the dosing orifices, 2) the displacement of gas in the unsaturated porous media by large volume doses and 3) the release of large concentrations of dissolved gases when the gas-liquid surface area increases in unsaturated or aerated systems.

4.3.3. Carbon dioxide

The CO2 flux from the first stage was 59 % lower than the second stage flux, even though 31 times more COD was removed in the first stage (combined daily load of influent and recycle doses) than the second stage (Table 1). Emissions from the first stage are lower than and emissions from the second stage were greater than the COD removed from each stage on a mass carbon basis, respectively (assuming 0.33 g C per g COD, Dubber and Gray, 2010). This strongly suggests that CO2 flux measured from each stage was not representative of the overall heterotrophic activity in that stage. The removal of COD in the first stage of the system confirms mineralization of organic carbon present in the influent wastewater by heterotrophic processes, including denitrification. However, the resulting inorganic carbon may be dissolved as carbonate species and not released as CO₂. Additionally, since CO₂ is highly soluble, significant quantities may have been transported with water to the second stage and off-gassed in the unsaturated second stage by mechanism 1 or mechanism 3 (Fig. 5). The second stage offers greater unsaturated surface area than the first stage, allowing for the volatilization of dissolved inorganic carbon due to interphase mass transfer (Doran, 1995). Additionally, nitrification in the second stage consumes alkalinity, resulting in a potentially lower pH and an increase of CO2 offgassing (Sharifian et al., 2021). Although pH and dissolved gases were not measured during the time of gas measurements in this study, future investigations should monitor pH and dissolved inorganic carbon to better understand carbonate system dynamics that contribute to emissions.

4.4. Temporal influence of hydraulic loading on first stage

The discrepancy in emissions due to pulse loading has the potential to skew observed fluxes depending on sampling strategy. The majority of studies utilize the static chamber method (Bruun et al., 2017; Johansson et al., 2004; Mander et al., 2011, 2014; Teiter and Mander, 2005; Tumendelger et al., 2019; Zhou et al., 2020), where singular

concentration measurements are taken periodically over the course of an hour as grab samples. The static chamber method of sampling is infrequent and is more suitable for long-term temporal observations over seasons and years, resulting in more smoothed emission trends. However, to observe the instantaneous influence of pulse or intermittent loading, a higher sampling frequency, as was completed in this study, is required to encompass the overall fluctuations of emissions. If the static chamber method is employed immediately after a dose, emissions may be falsely elevated, whereas samples taken hours later may be significantly lower. Both changes in microbial production and in mass transfer due to intermittent dosing can create variability in the observed emissions over a dosing schedule. However, further studies are required to separate the effect of each factor, and in systems such as TWs, these factors have complex and interrelated effects on emissions.

5. Conclusions

- 1. Emissions of CH_4 and N_2O were significantly higher in the first stage compared to the second stage of the TW (Table 1 & Fig. 2). As a result, our initial hypothesis that emissions between processes would be similar is not supported, nor can we effectively attribute differences in emissions directly to changes in nitrification or denitrification. Chamber temperature was correlated with N_2O and CO_2 emissions, but not CH_4 emissions.
- 2. CO₂ emissions were nearly 2.5 times higher in the second stage despite low organic carbon loading (Table 1 & Fig. 2). The discrepancies in the carbon balance are hypothesized to be the result of dissolved inorganic carbon produced in the first stage that are then off-gassing in the second stage. Future research should more thoroughly track the carbon balance of the system.
- 3. We hypothesized a dynamic behavior of N₂O, CH₄ and CO₂ emissions due to intermittent hydraulic loading. Data confirmed statistically significant patterns in emissions that emerged with hydraulic loading (Fig. 4). However, these patterns pointed more strongly to the

- impacts of convective transport and mass transfer rather than microbial production. Median emissions were within the range of other studied systems; however, the findings justify the need for more frequent sampling to avoid over- or underestimating overall emissions due to pulse loading of TW systems. Accurate estimations of emissions and GWP are essential for inventory tracking and future mitigation of GHGs.
- 4. Without being able to effectively track biogenic and abiotic sources of emissions, it is difficult to effectively develop methods for GHG mitigation. Future research should more thoroughly account for dissolved concentrations and system mass balances of carbon and nitrogen to determine whether flux rates can be attributed to microbial production within the system or to mass transfer.
- 5. The emission factors for N₂O and CH₄ were similar to similarly operated TW systems and on the low end of most other treatment processes, suggesting that TWs have a lower environmental impact than most mechanical WWTPs. Some of these differences may be due to the method in which EF was calculated.

Funding

This work was supported by the Bridger Bowl Foundation; the National Science Foundation Research Traineeship [award no. 2125748]; the Benjamin Fellowship through Montana State University's Norm Asbjornson College of Engineering (MSU NACOE); and the Montana Department of Environmental Quality under the State Revolving Fund (SRF) [contract no. 221031].

CRediT authorship contribution statement

S.H. Ayotte: Conceptualization, Data curation, Formal analysis, Methodology, Validation, Writing – original draft, Writing – review & editing, Investigation. **C.R. Allen:** Conceptualization, Data curation, Funding acquisition, Methodology, Writing – review & editing, Investigation. **A. Parker:** Formal analysis, Writing – review & editing. **O.R. Stein:** Conceptualization, Funding acquisition, Methodology, Resources, Supervision, Writing – review & editing. **E.G. Lauchnor:** Conceptualization, Funding acquisition, Methodology, Resources, Supervision, Writing – review & editing.

Declaration of competing interest

The authors declare that they have no known competing financial interests or personal relationships that could have appeared to influence the work reported in this paper.

Data availability

Data will be made available on request.

Acknowledgement

We thank the following entities and individuals for their financial and personal support of this project: the Montana Department of Environmental Quality, especially Paul Lavigne; Bridger Bowl Inc., especially Erik Pidgeon; and graduate students Kristen Brush, Justin Gay and Bryce Currey. We give special thanks to Drs Anthony Hartshorn and Elan (Jack) Brookshire who both so kindly provided the equipment that allowed us to analyze GHG emissions from our treatment wetland.

Appendix. Supplementary data

Supplementary data to this article can be found online at https://doi. org/10.1016/j.scitotenv.2024.171484.

References

- Allen, C.R., 2016. Nitrogen Removal and Associated Greenhouse Gas Production in Laboratory-Scale Treatment Wetlands.
- Altor, A.E., Mitsch, W.J., 2008. Methane and carbon dioxide dynamics in wetland mesocosms: effects of hydrology and soils. Ecol. Appl. 18, 1307–1320. https://doi. org/10.1890/07-0009.1.
- Armstrong, W., 2000. Oxygen distribution in wetland plant roots and permeability barriers to gas-exchange with the rhizosphere: a microelectrode and modelling study with Phragmites australis. Ann. Bot. 86, 687–703. https://doi.org/10.1006/apbp.2000.1236.
- Bahram, M., Espenberg, M., Pärn, J., Lehtovirta-Morley, L., Anslan, S., Kasak, K., Köljalg, U., Liira, J., Maddison, M., Moora, M., Niinemets, Ü., Öpik, M., Pärtel, M., Soosaar, K., Zobel, M., Hildebrand, F., Tedersoo, L., Mander, Ü., 2022. Structure and function of the soil microbiome underlying N2O emissions from global wetlands. Nat. Commun. 13, 1–10. https://doi.org/10.1038/s41467-022-29161-3.
- Bridger Bowl Inc, 2023. Weather History. Alpine Weather Station, Bridger Bowl, MT.
- Bruun, J., Hoffmann, C.C., Kjaergaard, C., 2017. Convective transport of dissolved gases determines the fate of the greenhouse gases produced in reactive drainage filters. Ecol. Eng. 98, 1–10. https://doi.org/10.1016/j.ecoleng.2016.10.027.
- Campos, J.L., Valenzuela-Heredia, D., Pedrouso, A., Val del Río, A., Belmonte, M., Mosquera-Corral, A., 2016. Greenhouse gases emissions from wastewater treatment plants: minimization, treatment, and prevention. J. Chem. 2016, 1–12. https://doi. org/10.1155/2016/3796352.
- Cavanaugh, S.K., 2021. Nitrous oxide emissions from wastewater treatment and process parameters affecting emissions. Master's Thesis. University of Washington.
- Chen, H., Zeng, L., Wang, D., Zhou, Y., Yang, X., 2020a. Recent advances in nitrous oxide production and mitigation in wastewater treatment. Water Res. 184, 116168 https://doi.org/10.1016/j.watres.2020.116168.
- Chen, X., Zhu, H., Yan, B., Shutes, B., Tian, L., Wen, H., 2020b. Optimal influent COD/N ratio for obtaining low GHG emissions and high pollutant removal efficiency in constructed wetlands. J. Clean. Prod. 267, 122003 https://doi.org/10.1016/j.jclepro.2020.122003.
- Croghan, C., Egeghy, P., 2003. Methods of dealing with values below the limit of detection using SAS. US-EPA. https://api.semanticscholar.org/CorpusID:12446551.
- Doran, P.M., 1995. Mass Transfer, in: Bioprocess Engineering Principles. Elselvier Science & Technology, pp. 190–217.
- Dotro, G., Langergraber, G., Molle, P., Nivala, J., Puigagut, J., Stein, O., von Sperling, M., 2017. Treatment wetlands. IWA Publishing. https://doi.org/10.2166/9781780408774
- Duan, H., Wang, Q., Erler, D.V., Ye, L., Yuan, Z., 2018. Effects of free nitrous acid treatment conditions on the nitrite pathway performance in mainstream wastewater treatment. Sci. Total Environ. 644, 360–370. https://doi.org/10.1016/j. scitotenv.2018.06.346.
- Dubber, D., Gray, N.F., 2010. Replacement of chemical oxygen demand (COD) with total organic carbon (TOC) for monitoring wastewater treatment performance to minimize disposal of toxic analytical waste. J. Environ. Sci. Health Part A 45, 1595–1600. https://doi.org/10.1080/10934529.2010.506116.
- Eilers, P.H.C., Marx, B.D., 1996. Flexible smoothing with B-splines and penalties. Stat. Sci. 11 https://doi.org/10.1214/ss/1038425655.
- EPA, 2022. Inventory of U.S. Greenhouse Gas Emissions and Sinks: 1990–2020. (No. EPA 430-R-22-003). U.S. Environmental Protection Agency.
- Faulwetter, J.L., Gagnon, V., Sundberg, C., Chazarenc, F., Burr, M.D., Brisson, J., Camper, A.K., Stein, O.R., 2009. Microbial processes influencing performance of treatment wetlands: a review. Ecol. Eng. 35, 987–1004. https://doi.org/10.1016/j. ecoleng.2008.12.030.
- Faulwetter, J.L., Burr, M.D., Parker, A.E., Stein, O.R., Camper, A.K., 2013. Influence of season and plant species on the abundance and diversity of sulfate reducing Bacteria and Ammonia oxidizing Bacteria in constructed wetland microcosms. Microb. Ecol. 65, 111–127. https://doi.org/10.1007/s00248-012-0114-y.
- Fernández-Baca, C.P., Truhlar, A.M., Omar, A.E.H., Rahm, B.G., Walter, M.T., Richardson, R.E., 2018. Methane and nitrous oxide cycling microbial communities in soils above septic leach fields: abundances with depth and correlations with net surface emissions. Sci. Total Environ. 640–641, 429–441. https://doi.org/10.1016/j. scitotenv.2018.05.303.
- Foley, J., de Haas, D., Yuan, Z., Lant, P., 2010. Nitrous oxide generation in full-scale biological nutrient removal wastewater treatment plants. Water Res. 44, 831–844. https://doi.org/10.1016/j.watres.2009.10.033.
- Harville, D.A., 2023. Maximum Likelihood Approaches to Variance Component Estimation and to Related Problems.
- Hastie, Trevor, Tibshirani, Robert, 1986. Generalized additive models. Stat. Sci. 1, 297–318.
- Henze, M. (Ed.), 2008. Biological Wastewater Treatment: Principles, Modeling and Design. IWA Pub, London.
- Hernandez, M.E., Mitsch, W.J., 2006. Influence of hydrologic pulses, flooding frequency, and vegetation on nitrous oxide emissions from created riparian marshes. Wetlands 26, 862–877. https://doi.org/10.1672/0277-5212(2006)26[862:IOHPFF]2.0.CO;2.
- Hernandez, M.E., Mitsch, W.J., 2007. Denitrification in created riverine wetlands: influence of hydrology and season. Ecol. Eng. 30, 78–88. https://doi.org/10.1016/j.ecoleng.2007.01.015.
- Hernández, M.E., Galindo-Zetina, M., Juan Carlos, H.-H., 2018. Greenhouse gas emissions and pollutant removal in treatment wetlands with ornamental plants under subtropical conditions. Ecol. Eng. 114, 88–95. https://doi.org/10.1016/j. ecoleng.2017.06.001.
- IPCC, 2019. Climate Change and Land: an IPCC special report on climate change, desertification, land degradation, sustainable land management, food security, and

- greenhouse gas fluxes in terrestrial ecosystems [P.R. Shukla, J. Skea, E. Calvo Buendia, V. Masson-Delmotte, H.-O. Pörtner, D. C. Roberts, P. Zhai, R. Slade, S. Connors, R. van Diemen, M. Ferrat, E. Haughey, S. Luz, S. Neogi, M. Pathak, J. Petzold, J. Portugal Pereira, P. Vyas, E. Huntley, K. Kissick, M. Belkacemi, J. Malley, (eds.)].Refinement to the 2006 IPCC Guidelines for National Greenhouse Gas Inventories. Guidelines for National Greenhouse Gas Inventories. International Panel on Climate Change (IPCC).
- IPCC, 2021. Climate Change 2021 The Physical Science Basis: Working Group I Contribution to the Sixth Assessment Report of the Intergovernmental Panel on Climate Change, 1st ed. Cambridge University Press, Cambridge, United Kingdom and New York, NY USA. https://doi.org/10.1017/9781009157896.
- Ji, B., Chen, J., Li, W., Mei, J., Yang, Y., Chang, J., 2021. Greenhouse gas emissions from constructed wetlands are mitigated by biochar substrates and distinctly affected by tidal flow and intermittent aeration modes. Environ. Pollut. 271, 116328 https:// doi.org/10.1016/j.envpol.2020.116328.
- Jiang, X., Tian, Y., Ji, X., Lu, C., Zhang, J., 2020. Influences of plant species and radial oxygen loss on nitrous oxide fluxes in constructed wetlands. Ecol. Eng. 142, 105644 https://doi.org/10.1016/j.ecoleng.2019.105644.
- Johansson, A.E., Gustavsson, A.-M., Öquist, M.G., Svensson, B.H., 2004. Methane emissions from a constructed wetland treating wastewater—seasonal and spatial distribution and dependence on edaphic factors. Water Res. 38, 3960–3970. https:// doi.org/10.1016/j.watres.2004.07.008.
- Kasak, K., Kill, K., Uuemaa, E., Maddison, M., Aunap, R., Riibak, K., Okiti, I., Teemusk, A., Mander, Ü., 2022. Low water level drives high nitrous oxide emissions from treatment wetland. J. Environ. Manag. 312, 114914 https://doi.org/10.1016/j. jenvman.2022.114914.
- Kaushal, S.S., Mayer, P.M., Vidon, P.G., Smith, R.M., Pennino, M.J., Newcomer, T.A., Duan, S., Welty, C., Belt, K.T., Sujay, S., Mayer, P.M., Vidon, P.G., Smith, R.M., Pennino, M.J., New-, T.A., Duan, S., Welty, C., Belt, K.T., Use, L., Amplify, C.V., 2014. Land Use And Climate Variability Amplify Carbon, Nutrient, And Contaminant Pulses: A Review With Management Implications, 1 50, pp. 585–614. https://doi. org/10.1111/jawr.12204.
- Law, Y., Ye, L., Pan, Y., Yuan, Z., 2012. Nitrous oxide emissions from wastewater treatment processes. Philos. Trans. R. Soc. B Biol. Sci. 367, 1265–1277. https://doi. org/10.1098/rstb.2011.0317.
- Livingston, G.P., Hutchinson, G.L., Spartalian, K., 2006. Trace gas emission in chambers: a non-steady-state diffusion model. Soil Sci. Soc. Am. J. 70, 1459–1469. https://doi. org/10.2136/sssaj2005.0322.
- Ma, W.K., Farrell, R.E., Siciliano, S.D., 2011. Nitrous oxide emissions from ephemeral wetland soils are correlated with microbial community composition. Front. Microbiol. 2, 1–11. https://doi.org/10.3389/fmicb.2011.00110.
- Mander, Ü., Löhmus, K., Teiter, S., Mauring, T., Nurk, K., Augustin, J., 2008. Gaseous fluxes in the nitrogen and carbon budgets of subsurface flow constructed wetlands. Sci. Total Environ. 404, 343–353. https://doi.org/10.1016/j.scitotenv.2008.03.014.
- Mander, Ü., Maddison, M., Soosaar, K., 2011. The impact of pulsing hydrology and fluctuating water table on greenhouse gas emissions from constructed. Wetlands 4, 1023–1032. https://doi.org/10.1007/s13157-011-0218-z.
- Mander, Ü., Dotro, G., Ebie, Y., Towprayoon, S., Chiemchaisri, C., Furlan, S., Jamsranjav, B., Kasak, K., Truu, J., Tournebize, J., Mitsch, W.J., 2014. Greenhouse gas emission in constructed wetlands for wastewater treatment: a review. Ecol. Eng. 66. 19–35. https://doi.org/10.1016/j.ecoleng.2013.12.006.
- 66, 19–35. https://doi.org/10.1016/j.ecoleng.2013.12.006.

 Mander, Ü., Tournebize, J., Espenberg, M., Chaumont, C., Torga, R., Garnier, J.,
 Muhel, M., Maddison, M., Lebrun, J.D., Uher, E., Remm, K., Pärn, J., Soosaar, K.,
 2021. High denitrification potential but low nitrous oxide emission in a constructed
 wetland treating nitrate-polluted agricultural run-off. Sci. Total Environ. 779,
 146614 https://doi.org/10.1016/j.scitotenv.2021.146614.
- Maucieri, C., Borin, M., Milani, M., Cirelli, G.L., Barbera, A.C., 2019. Plant species effect on CO2 and CH4 emissions from pilot constructed wetlands in Mediterranean area. Ecol. Eng. 134, 112–117. https://doi.org/10.1016/j.ecoleng.2019.04.019.
- Metcalf & Eddy, Inc, Tchobanoglous, G., Stensel, H.D., Tsuchihashi, R., Burton, F.L., 2014. Wastewater Engineering: Treatment and Resource Recovery, 5th ed. McGraw
- Meyer, R.L., Zeng, R.J., Giugliano, V., Blackall, L.L., 2005. Challenges for simultaneous nitrification, denitrification, and phosphorus removal in microbial aggregates: mass transfer limitation and nitrous oxide production. FEMS Microbiol. Ecol. 52, 329–338. https://doi.org/10.1016/j.femsec.2004.11.011.
- Nakazawa, T., Matsuno, T., 2020. Current understanding of the global cycling of carbon dioxide, methane, and nitrous oxide. Proc. Jpn. Acad. Ser. B Phys. Biol. Sci. 96, 394–419. https://doi.org/10.2183/pjab.96.030.

- Oertel, C., Matschullat, J., Zurba, K., Zimmermann, F., Erasmi, S., 2016. Greenhouse gas emissions from soils—a review. Geochemistry 76, 327–352. https://doi.org/10.1016/j.chemer.2016.04.002.
- Pan, Y., van den Akker, B., Ye, L., Ni, B.-J., Watts, S., Reid, K., Yuan, Z., 2016. Unravelling the spatial variation of nitrous oxide emissions from a step-feed plug-flow full scale wastewater treatment plant. Sci. Rep. 6, 20792 https://doi.org/ 10.1038/srep.20792.
- R Core Team, 2022. R: A language and environment for statistical computing.
- Reay, D.S., Davidson, E.A., Smith, K.A., Smith, P., Melillo, J.M., Dentener, F., Crutzen, P. J., 2012. Global agriculture and nitrous oxide emissions. Nat. Clim. Chang. 2, 410–416. https://doi.org/10.1038/nclimate1458.
- Rhine, E.D., Mulvaney, R.L., Pratt, E.J., Sims, G.K., 1998. Improving the Berthelot reaction for determining ammonium in soil extracts and water. Soil Sci. Soc. Am. J. 62, 473. https://doi.org/10.2136/sssaj1998.03615995006200020026x.
- Rodriguez-Caballero, A., Aymerich, I., Marques, R., Poch, M., Pijuan, M., 2015. Minimizing N2O emissions and carbon footprint on a full-scale activated sludge sequencing batch reactor. Water Res. 71, 1–10. https://doi.org/10.1016/j. watres.2014.12.032.
- Shammas, N.K., 1986. Interactions of temperature, pH, and biomass on the nitrification process. Wiley 58, 52–59.
- Sharifian, R., Wagterveld, R.M., Digdaya, I.A., Xiang, C., Vermaas, D.A., 2021.
 Electrochemical carbon dioxide capture to close the carbon cycle. Energy Environ.
 Sci. 14, 781–814. https://doi.org/10.1039/D0EE03382K.
- Teiter, S., Mander, Ü., 2005. Emission of N2O, N2, CH4, and CO2 from constructed wetlands for wastewater treatment and from riparian buffer zones. Ecol. Eng. 25, 528–541. https://doi.org/10.1016/j.ecoleng.2005.07.011.
- Tumendelger, A., Alshboul, Z., Lorke, A., 2019. Methane and nitrous oxide emission from different treatment units of municipal wastewater treatment plants in Southwest Germany. PLoS One 14, e0209763. https://doi.org/10.1371/journal.pone.0209763.
- Velthuis, M., Veraart, A.J., 2022. Temperature sensitivity of freshwater denitrification and N 2 O emission—a Meta-analysis. Global Biogeochem. Cycles 36, 1–14. https:// doi.org/10.1029/2022gb007339.
- Verboven, P., Pedersen, O., Ho, Q.T., Nicolai, B.M., Colmer, T.D., 2014. The mechanism of improved aeration due to gas films on leaves of submerged rice: leaf gas films on submerged rice. Plant Cell Environ. n/a-n/a. https://doi.org/10.1111/pce.12300.
- Vilain, G., Garnier, J., Decuq, C., Lugnot, M., 2014. Nitrous oxide production from soil experiments: denitrification prevails over nitrification. Nutr. Cycl. Agroecosyst. 98, 169–186. https://doi.org/10.1007/s10705-014-9604-2.
- Wang, H., Sun, Y., Wu, G., Guan, Y., 2019. Effect of anoxic to aerobic duration ratios on nitrogen removal and nitrous oxide emission in the multiple anoxic/aerobic process. Environ. Technol. U. K. 40, 1676–1685. https://doi.org/10.1080/ 09593330.2018.1427801.
- Western Agricultural Research Center, 2019. Summary of Montana Growing Conditions [WWW Document]. Summ. Mont. Grow. Conditions West. Agric. Res. Cent. Mont. State Univ. URL. https://agresearch.montana.edu/warc/guides/summary_of_Montana_growing_conditions.html#:~:text=Montana%20has%20a%20short%20growing,frost%2Dfree%20days%20on%20average (accessed 1.31.24).
- Wood, S.N., 2011. Fast stable restricted maximum likelihood and marginal likelihood estimation of semiparametric generalized linear models. J. R. Stat. Soc. B 73, 3–36.
 Wood, S.N., 2017. Generalized Additive Models: An Introduction with R, 2nd ed. CRC
- Wunderlin, P., Mohn, J., Joss, A., Emmenegger, L., Siegrist, H., 2012. Mechanisms of N2O production in biological wastewater treatment under nitrifying and denitrifying conditions. Water Res. 46, 1027–1037. https://doi.org/10.1016/j. watres.2011.11.080.
- Zhou, N., Dang, C., Zhao, Z., He, S., Zheng, M., Liu, W., Wang, X., 2019. Role of sludge retention time in mitigation of nitrous oxide emission from a pilot-scale oxidation ditch. Bioresour. Technol. 292, 121961 https://doi.org/10.1016/j. biortech.2019.121961.
- Zhou, S., Wang, C., Liu, C., Sun, H., Zhang, J., Zhang, X., Xin, L., 2020. Nutrient removal, methane and nitrous oxide emissions in a hybrid constructed wetland treating anaerobic digestate. Sci. Total Environ. 733, 138338 https://doi.org/10.1016/j.scitotenv.2020.138338.
- Zhu-Barker, X., Cavazos, A.R., Ostrom, N.E., Horwath, W.R., Glass, J.B., 2015. The importance of abiotic reactions for nitrous oxide production. Biogeochemistry 126, 251–267. https://doi.org/10.1007/s10533-015-0166-4.